Supporting Information

Shin et al. 10.1073/pnas.1304996110

SI Materials and Methods

Cell Culture. Fresh purified bone marrow-derived human $CD34^+$ cells and total mononuclear cells were obtained from either the Penn Xenograft Core Facility or AllCells (Emeryville, CA). Cells from at least five different donors were used in this study. Purity of the samples (>98%) was confirmed by flow cytometry with monoclonal antibody against human CD34. All experiments with primary cells were performed in primary hematopoietic media (StemLine-II; Sigma) supplemented with 1× antibiotics and the following human recombinant cytokines: stem cell factor (SCF; 100 ng/mL) and thrombopoietin (Tpo; 100 ng/mL). In some occasions, the media were also supplemented by fetal bovine serum (FBS) [10% (vol/vol)], dexamethasone (Sigma; 1 μM), 17β-estradiol (Sigma; 1 μM), granulocyte-colony stimulating factor (G-CSF; 10 ng/mL), erythropoietin (EPO; 1 U/mL), and interleukin-3 (IL-3, 1 ng/mL). All cytokines were purchased from R&D Systems. MEG01 and COS-1 cells were cultured in RPMI-1640 and DMEM, respectively, supplemented with 10% FBS and 1% antibiotics. In some cases, cells were treated with different doses of drugs after 7∼10 d of culture, including all-trans retinoic acid (RA) (Sigma), AGN 193109 (Santa Cruz Biotechnology), 17-(Allylamino)-17-demethoxygeldanamycin (17-AAG; Sigma), and anacardic acid (Sigma) for indicated durations of up to 3 d. Cells were cultured at 37 °C in 5% CO_2.

Mass Spectrometry-Calibrated Intracellular Flow Cytometry. Cells were fixed with 4% paraformaldehyde in PBS for 10 min, washed with PBS/1% BSA (staining medium), and incubated in 0.5% Triton X-100 for 10 min. After washing with the staining medium, samples were stained with antibodies against cytoplasmic antigens, including rabbit anti–lamin-A and goat anti–lamin-B (all from Santa Cruz Biotechnology) for 1 h at room temperature. In addition, cells were concurrently stained with Hoechst 33342 (Invitrogen) and lineage markers, including the following: phycoerythrin (PE) or APC (allophycocyanin)-Cy7 anti-CD34 (581; Invitrogen or Biolegend), PECy7 anti-CD38 (HIT2; eBioscience), PE anti-human CD33, PE anti-human CD19, PE anti-human CD3 (all from Biolegend), PE or APC anti-human glycophorin A (GPA) (Invitrogen), and FITC or APC anti-human CD41 (eBioscience). Cells were then washed and stained with anti-rabbit Alexa 488 and anti-goat Alexa 647 (Invitrogen) for 30 min, followed by analysis on LSR II flow cytometer (Becton Dickinson).

After intracellular flow cytometry to obtain the mean fluorescent intensity (MFI) values of lamin-A and lamin-B across different samples, each MFI value from flow cytometry was calibrated against mass spectrometry results with A549. From flow cytometry:

$$[A]_{\mathrm{A549}} \cdot \alpha = I^A_{\mathrm{A549}}$$
$$[B]_{\mathrm{A549}} \cdot \beta = I^B_{\mathrm{A549}},$$

where $[A]$ and $[B]$ represent concentrations of lamins A and B, α and β are instrument response functions (in this case, direct proportionality), and I is the mean fluorescence intensity in either lamin channel from flow cytometry. From mass spectrometry, the absolute ratio between isoforms is defined as R.

$$\frac{[A]_{\mathrm{A549}}}{[B]_{\mathrm{A549}}} = R_{\mathrm{A549}}$$

The estimate of R_{A549} is 2.3. Combine instrument response functions into k, which can be defined from experimentally measureable terms (using A549 as a standard):

$$\frac{\alpha}{\beta} = \frac{I^A_{\mathrm{A549}}}{I^B_{\mathrm{A549}} \cdot R_{\mathrm{A549}}} = k,$$

k = 0.26. Other samples can then be characterized from flow cytometry measurements, based on calibration through this scaling factor:

$$\frac{[A]_x}{[B]_x} = \frac{I^A_x}{I^B_x \cdot k}$$
$$[A]_x + [B]_x = \frac{I^A_x}{\alpha} + \frac{I^B_x}{\beta} = \beta^{-1} \cdot \left(\frac{I^A_x}{k} + I^B_x\right)$$
$$[A]_x + [B]_x \propto \left(\frac{I^A_x}{k} + I^B_x\right).$$

Western Blot Analysis. Cells were washed with ice-cold PBS and lysed on ice with lysis buffer (150 mM sodium chloride, 1% Nonidet P-40, 1% protease inhibitor mixture 50 mM Tris at pH 8.0) mixed with 1× NUPAGE LDS sample buffer (Invitrogen) for 30 min with sonication. Samples were then boiled for 10 min at 90∼100 °C, followed by centrifugation for 5 min at 11,200 × g. For Western blot, whole lysates were separated on 3–7% NUPAGE Tris-Acetate gels (Invitrogen). The proteins were then transferred to a polyvinylidene fluoride (PVDF) membrane with an iBlot Gel Transfer Device (Invitrogen), followed by blocking with 5% nonfat dry milk solution for 1 h. Incubation with primary antibodies was done at 4 °C overnight with 1:1,000 total rabbit anti–lamin-A or goat anti–lamin-B (Santa Cruz Technology). After washing, the membrane was incubated with 1:2,500 anti-rabbit and 1:1,000 anti-goat HRP-conjugated IgG antibodies at room temperature for 1 h. The blot was developed with ChromoSensor (GenScript) for 5 min, followed by digital scanning to perform densitometry analysis by ImageJ (National Institutes of Health).

Micropipette Analysis. Primary cells or cell lines in suspension were subjected to micropipette analysis. Capillary tubes of 1.0 mm inner diameter (World Precision Instruments) were pulled into micropipettes using a Flaming-Brown Micropipette Puller (Sutter Instrument) and cut further using a deFonbrune-type microforge (Vibratome). The average micropipette diameter was around 3 μm. Micropipettes were attached to a dual-stage water manometer with reservoirs of adjustable height. Suction was applied by a syringe, and the corresponding pressure was measured by pressure transducer (Validyne) calibrated by a mercury U-tube manometer. Pressures for different experiments ranged from 0.5 to 15 kPa.

Pore-Migration Assay. Migration of hematopoietic cells was measured in a modified Boyden chamber migration assay using Transwell inserts with a 3-, 5-, and 8-μm porous membrane (Millipore). Cells were loaded into the migration chamber in a serum-free condition. Medium containing 100 ng/mL stromal derived factor-1 (SDF-1) (Peprotech) was placed in the lower chamber in some studies. After allowing cell migration for 4 h, cells were removed from the lower chamber as well as the upper side of membranes. The number and type of migratory cells were evaluated by flow cytometry with defined number of fluorescent beads (APC conjugated, Becton Dickinson) and staining cells with lineage markers as used in mass spectrometry-calibrated intracellular flow (MS-IF) cytometry. To evaluate the effect of drugs or RNAi of lamins on migration, cells were pretreated with RA, lamin-A

siRNA, or lamin-B shRNA for 3 d before loading onto the migration chamber.

Introduction of Nucleic Acids in Vitro. $CD34^+$-derived cells or MEG01 cells were transfected with GFP-lamin-A (wild-type or mutants) or lamin-A siRNA by electroporation ("nucleofection") using the Nucleofector kits (Lonza) as described in the manual. Briefly, cultured cells were washed with PBS and resuspended with transfection solution containing 2 μg/mL DNA constructs or 3 μg/mL siRNA. They were then transferred into a cuvette and transfected with the Nucleofector II. The medium at 37 °C was then added to transfected cells. Cells were incubated overnight, and then the medium was exchanged to fresh on the next day.

To silence the expression of lamin-B1, the retrovirus vector constructs containing shRNA were obtained from the laboratory of Robert Goldman (Northwestern University, Chicago) and prepared as described previously (1). pSilencer constructs containing either scrambled or lamin-B1 shRNA sequences were transfected into HEK-293T cells, and virus-containing culture supernatants were collected at 24~48 h following transfection in serum-free hematopoietic media. The culture supernatants containing virus were then incubated with $CD34^+$-derived cells for shRNA transduction in the presence of 5 μg/mL polybrene (Sigma) and incubated for 1 d. Virally transduced cells were selected by adding 1 μg/mL puromycin (Invitrogen) for 2 d and incubated in fresh medium for at least 1 d before further analyses. Lamin-A was also down-regulated stably in a similar manner as lamin-B1 with human lamin-A shRNA (Sigma).

For lamin-A promoter assays, we used a GFP construct driven by the human lamin-A promoter cloned by Genecopoeia. The promoter was derived from the 1,132-base pair upstream region and the first 385-base pair mRNA transcript region. Promoter activity was characterized with or without retinoic acid after transient transfection using LF2k (Invitrogen) per the manufacturer's instructions.

Colony-Forming Assay. One thousand to 3,000 $CD34^+$-derived cells were seeded into methylcellulose-containing media (MethoCult H4434; StemCell Technologies) supplemented with SCF, GM-CSF, IL-3, and Epo. They were cultured for 14 d, and colonies were scored at 10× magnification based on the published morphological criteria by StemCell Technoloigies. Colony-forming content was normalized per 10,000 cells seeded.

Image Acquisition and Analysis. Cells on coverslips were fixed with 4% paraformaldehyde, followed by permeabilization with 0.5% Triton X-100 in PBS for 15 min and blocking with 1% BSA in PBS for 30 min. Samples were then stained with primary antibodies (1:100 for all antibodies used) for overnight at 4 °C. After washing, staining with appropriate Alexa 488 or 647-conjugated secondary antibodies (1:400) and TRITC-phalloidin was performed for 45 min at room temperature. Cells were washed three times with PBS and mounted in ProLong Gold antifade medium (Invitrogen). Samples were then analyzed by fluorescence or confocal microscopy.

Live Cell Imaging Analysis. Cells transfected with GFP-lamin-A were put into Ibidi μ-slide VI (Ibidi GmbH) in cell-culture medium. Analysis was done in an insulated chamber maintained at 37 °C, 5% CO_2. A series of images were collected every 5 min for ~18 h with an Olympus IX70 inverted microscope with 300W Xenon lamp illumination using 20× objectives under bright field and fluorescence. Image stacks were further analyzed by ImageJ to analyze lamin-A distribution during polyploidization.

Mass Spectrometry Analysis of Posttranslational Modification. Sample preparation and subsequent analysis by mass spectrometry were performed in duplicate. Gel electrophoresis was performed as described previously. Gel sections were washed [50% 0.2 M ammonium bicarbonate (AB) solution, 50% acetonitrile (ACN), 30 min at 37 °C], dried by lyophilization, incubated with a reducing agent [20 mM Tris(2-carboxyethyl)phosphine (TCEP) in 25 mM AB solution at pH 8.0, 15 min at 37 °C], and alkylated [40 mM iodoacetamide (IAM) in 25 mM AB solution at pH 8.0, 30 min at 37 °C]. The gel sections were dried by lyophilization before in-gel trypsinization [20 μg/mL sequencing grade modified trypsin in buffer as described in the manufacturer's protocol (Promega), 18 h at 37 °C with gentle shaking]. The resulting solutions of tryptic peptides were acidified by addition of 50% digest dilution buffer (60 mM AM solution with 3% methanoic acid).

Peptide separations (5 μL injection volume) were performed on 25-cm PicoFrit column (75-μm inner diameter; New Objective) packed with Magic 3 μm C18 reversed-phase resin (Michrom Bioresources) using a nanoflow HPLCy system (Eksigent Technologies), which was coupled online to a hybrid LTQ-Orbitrap XL mass spectrometer (Thermo Fisher Scientific) via a nanoelectrospray ion source. Chromatography was performed with Solvent A (Milli-Q water with 0.1% formic acid) and Solvent B (acetonitrile with 0.1% formic acid). Peptides were eluted at 200 nL/min for 3–28% B over 42 min, 28–50% B over 26 min, 50–80% B over 5 min, 80% B for 4.5 min before returning to 3% B over 0.5 min. To minimize sample carryover, a fast blank gradient was run between each sample. The LTQ-Orbitrap XL was operated in the data-dependent mode to automatically switch between full scan MS (m/z = 300–2,000 in the orbitrap analyzer (with resolution of 60,000 at m/z 400) and the fragmentation of the six most intense ions by collision-induced dissociation in the ion trap mass analyzer.

Raw mass spectroscopy data were processed using Elucidator (version 3.3; Rosetta Biosoftware). The software was set up to align peaks in data from samples derived from corresponding molecular weight regions of the 1D gels. Peptide and protein annotations were made using SEQUEST (version 28; Thermo Fisher Scientific) with full tryptic digestion and up to two missed cleavage sites. Peptide masses were selected between 800 and 4,500 amu with peptide mass tolerance of 1.1 amu and fragment ion mass tolerance of 1.0 amu. Peptides were searched against databases compiled from UniRef100 (November 2010 database) human plus contaminants and a reverse decoy database. Only proteins detected with three or more peptides were considered for quantification. The peptide database was modified to search for alkylated cysteine residues (monoisotopic mass change, Δ = +57.021 Da), oxidized methionine (Δ = +15.995 Da), acetylated lysine (Δ = +42.011 Da), methylated lysine and arginine (Δ = +14.016 Da), and phosphorylated serine, tyrosine, threonine, histidine, and aspartate (Δ = +79.966 Da). The absolute ratio between protein isoforms (lamin A:B) was determined by consideration of peptides common to both forms, as described elsewhere (2). The relative signals of posttranslationally modified peptides were quantified as fractions of the average ion current of other peptides from the same parent protein.

Statistical Analyses. All statistical analyses were performed using GraphPad Prism 5. Unless noted, all statistical comparisons were made by unpaired 2-tailed Student t test and were considered significant if $P < 0.05$. Dose–response data were fit to sigmoidal dose–response of variable slope with x axis in a log scale.

Supplemental Discussion of Cortical Rigidity Versus Lamina Rigidity

The lamin expression pattern in our study is further supported by measurement of nuclear rheology. Very few studies have directly measured the mechanical properties of leukocyte nuclei. For lymphoid, one study suggests a nuclear cortical tension in T cells of ~2 mN/m (3), which is only twofold larger than the cortical tension required to fragment megakaryocytes (MKs) (2), consistent with the notion that lymphocytes down-regulate both lamin isoforms (Fig. 1*F*) and are highly deformable through pores (Fig. 2 and Fig. S3*B*). No cell intrinsic effect was observed in lymphocytes from lamin-A/C perturbed mice (4), consistent with low lamin levels.

Programming of cellular deformability during granulopoiesis has been suggested by micropipette (5) and microfluidic optical stretcher (6) methods, but these studies do not distinguish the contribution of cell cortex from that of the nucleus. Cortical stiffness is regulated by actomyosin forces via nonmuscle myosin-II (NMM-II) (7), and so we measure nuclear deformability in situ with latrunculin-A treatment to inhibit actomyosin forces (8). As demonstrated in the MK lineage, the expression of NMM-II is also dynamically regulated during terminal differentiation (2), which suggests that cortical deformability is also dynamically programmed in hematopoiesis. An obvious distinction here is that, whereas actin-myosin can generate force and contribute to "active" migration via adhesion and crawling, lamins are intermediate filaments that do not generate force, but their contributions to rigidity can limit migration. Relationships between nuclear and cortical elasticity in hematopoiesis need further study.

1. Shimi T, et al. (2011) The role of nuclear lamin B1 in cell proliferation and senescence. *Genes Dev* 25(24):2579–2593.
2. Shin JW, Swift J, Spinler KR, Discher DE (2011) Myosin-II inhibition and soft 2D matrix maximize multinucleation and cellular projections typical of platelet-producing megakaryocytes. *Proc Natl Acad Sci USA* 108(28):11458–11463.
3. Dong C, Skalak R, Sung KL (1991) Cytoplasmic rheology of passive neutrophils. *Biorheology* 28(6):557–567.
4. Hale JS, Frock RL, Mamman SA, Fink PJ, Kennedy BK (2010) Cell-extrinsic defective lymphocyte development in Lmna(-/-) mice. *PLoS ONE* 5(4):e10127.
5. Lichtman MA (1970) Cellular deformability during maturation of the myeloblast: Possible role in marrow egress. *N Engl J Med* 283(18):943–948.
6. Lautenschläger F, et al. (2009) The regulatory role of cell mechanics for migration of differentiating myeloid cells. *Proc Natl Acad Sci USA* 106(37):15696–15701.
7. Merkel R, et al. (2000) A micromechanic study of cell polarity and plasma membrane cell body coupling in Dictyostelium. *Biophys J* 79(2):707–719.
8. Pajerowski JD, Dahl KN, Zhong FL, Sammak PJ, Discher DE (2007) Physical plasticity of the nucleus in stem cell differentiation. *Proc Natl Acad Sci USA* 104(40):15619–15624.

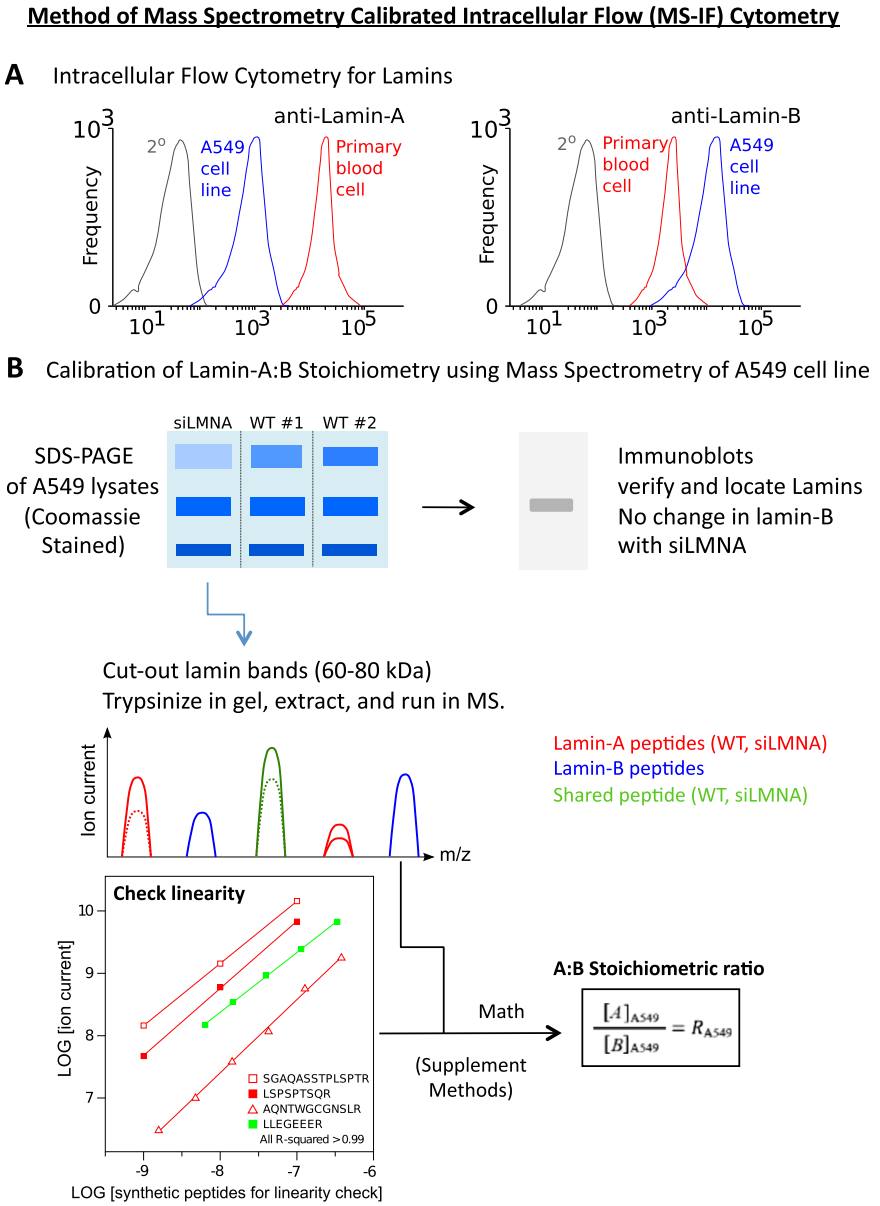

Fig. S1. Schematics of MS-IF-cytometry. (*A*) Representative plots showing lamin isoform expressions measured by intracellular flow cytometry. (*B*) Determination of absolute lamin-A:B ratios by calibrating flow cytometry results with mass spectometry. A549 was used as a standard. Detailed description is available in *SI Materials and Methods*.

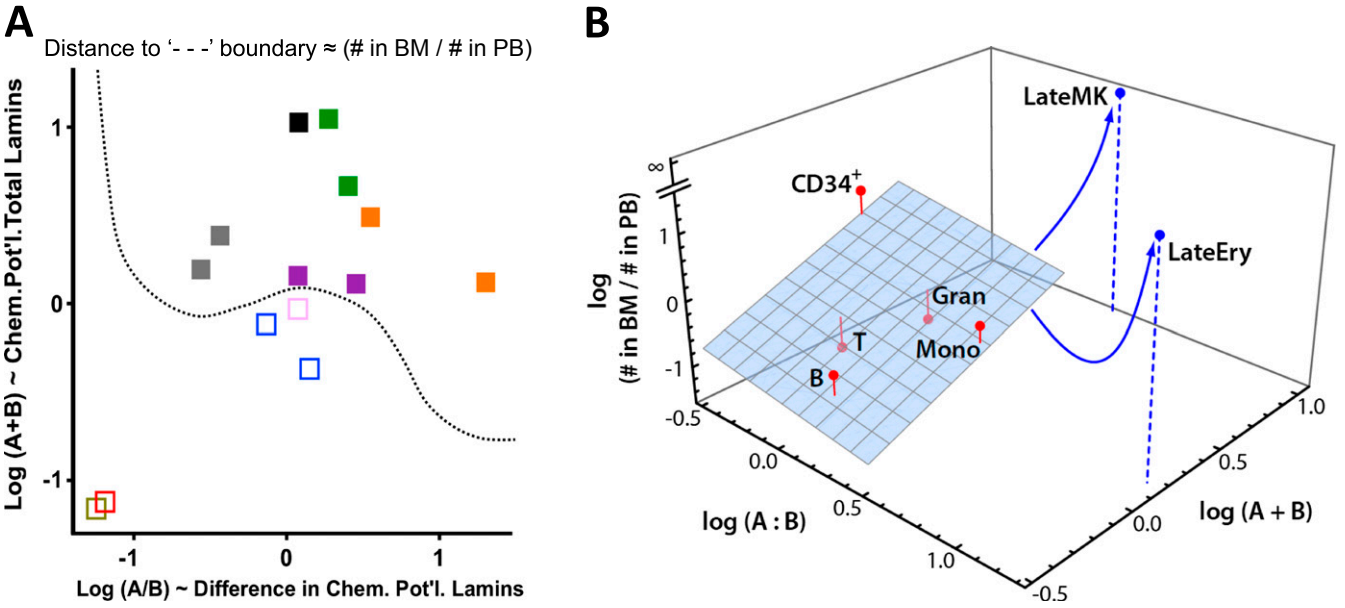

Fig. S2. Lamins and hematopoietic lineage distribution in marrow and blood. (*A*) Distribution of hematopoietic lineages expressed using the standard definition of chemical potential (Chem. Pot'l) as the logarithm of a relative concentration in a cell or nucleus. Distances from the curvilinear barrier to each point reflect known distribution of lineages between marrow and peripheral blood. (*B*) Log plot showing the relationship between lamin isoform ratio, total lamin intensity, and bone marrow (BM) to peripheral blood (PB) cell ratio. To formally assess the dependence of marrow/blood partitioning on the two coordinates of the lamin lineage map, literature values for known marrow-to-blood distributions were fitted for $CD34^+$, myeloid, and lymphoid lineages. Data from fresh $CD34^+$, T, B, granulocyte (Gran), and monocyte (Mono) were fit to a surface defined by the equation $z = A\,(x - b) + C\,(y - d)$ ($R^2 = 0.61$). Late MK and Late Ery are known to have very high BM:PB cell ratios and are not considered in the fit. Small deviations from a simple linear fit of the log data indicate that lamins contribute to compartmentalization of blood lineages.

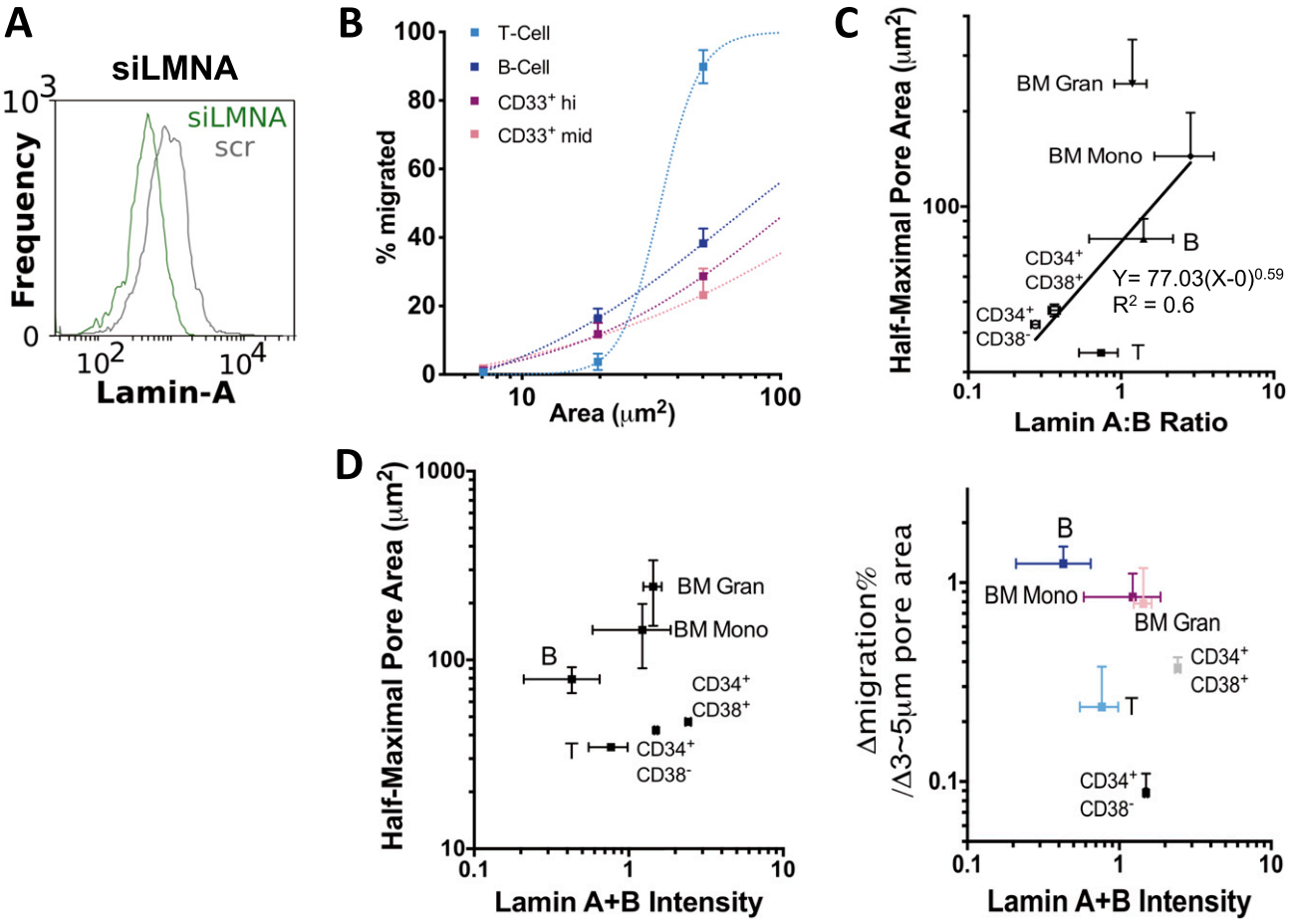

Fig. S3. 3D migration of hematopoietic lineages. (*A*) siRNA knockdown down-regulates lamin-A uniformly. Representative flow cytometry plot is shown. (*B*) Data from migration assays were fitted as in Fig. 2*B*, where A = 100 and (B, Xc, m): (T cell: 0.03, 1.44, 5.51), (B cell: 0.01, 6.64, 0.95), (CD33$^+$ hi, monocyte: 0.009, 5.00, 1.00), (CD33$^+$ mid, granulocyte, 0.005, 5.00, 0.79). (*C*) Correlation analysis between half-maximal pore area (μm^2) of migration ($A_{1/2}$) and lamin A:B ratios, where $A_{1/2} = Xc + 1/B$. See also Fig. 2*B*. The data were fitted with a power law, $Y = 77.03X^{0.59}$, $R^2 = 0.6$ for all data. (*D*, *Left*) Correlation analysis between $A_{1/2}$ and lamin total intensity. (*Right*) Correlation analysis between migration sensitivity, Y = Δ (% Migrated)/Δ (Pore Area) between 3- and 5-μm pores, and lamin total intensity. For all graphs, mean ± SEM of $n = 3$.

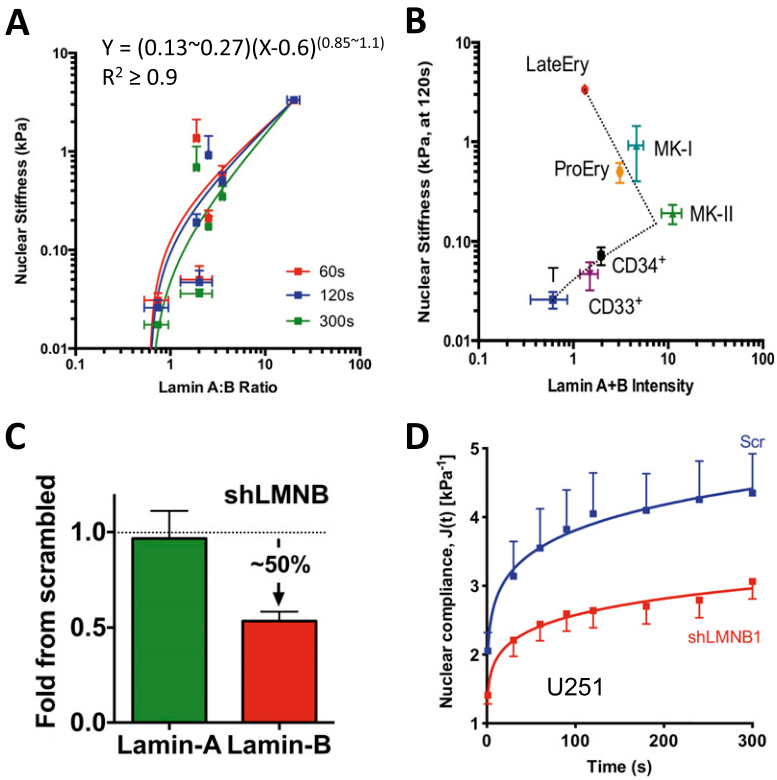

Fig. S4. Correlation analysis between nuclear stiffness and lamins. (*A*) Correlation between nuclear stiffness and lamin A:B ratio at 60, 120, and 300 s after aspiration under constant pressure. The graph was fitted with a power law, $Y = (0.13\sim0.27)(X\text{-}0.6)^{(0.85\sim1.1)}$, $R^2 \geq 0.9$. Mean ± SEM of $n \geq 5$ for each cell type. (*B*) Correlation analysis between nuclear stiffness and lamin total intensity at 120 s after aspiration. The graph was fitted with a power law, $Y = 0.05(X\text{-}0.32)^{0.55}$, $R^2 \geq 0.8$ for T cell, $CD33^+$, $CD34^+$, and MK-II, whereas $Y = 5.50X^{-1.80}$, $R^2 \geq 0.9$ for LateEry, ProEry, MK-I and MK-II. (*C*) Lamin-B shRNA down-regulates lamin-B without affecting lamin-A ($n = 3$ donors, $P < 0.05$). (*D*) Nuclear stiffening of U251 cells after lamin B1 knockdown. Nuclear compliance change with time under constant pressure $\Delta P \leq 3$ kPa over time with a power law fit, $J(t)$ (kPa^{-1}) = $A \cdot t^B$ (t = sec), where (A, B):): (scrambled (scr): 2.05, 0.13), (shLMNB1: 1.43, 0.13), $n = 5$, $P < 0.05$, scrambled vs. shLMNB1 at each time point, paired *t* test.

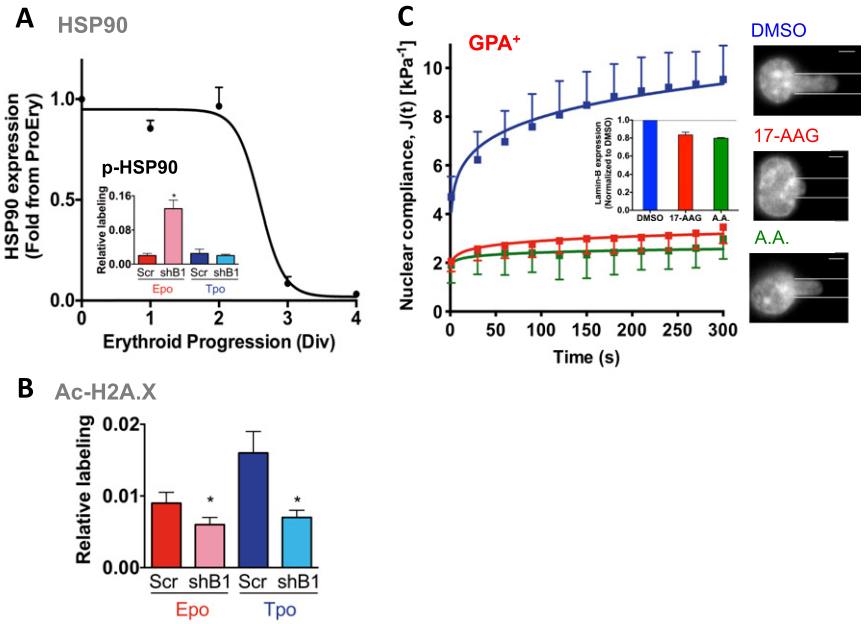

Fig. S5. Perturbation of physiological pathways can phenocopy the stiffening of nuclei with lamin-B down-regulation. Many other proteins change during erythropoiesis, and we hypothesized that, if we pharmacologically perturbed important erythropoietic pathways, then we should be able to phenocopy lamin-B changes as intrinsic to a common erythropoietic program. To first identify candidate targets, we performed quantitative mass spectrometry analyses of erythroid cells both without and with lamin-B1 RNAi treatment, which promotes BFU-Es. (*A*) HSP90 protein down-regulated during late erythropoiesis based on mass spectometry profiling of erythropoietic cells at five distinct stages of differentiation (1), consistent with a role for HSP90 in hematopoietic differentiation (2). (*Inset*) HSP90 phosphorylation levels at Ser226 and Ser255 (involved in drug resistance of cancer cells) (3) are up-regulated by lamin-B1 knockdown only in the presence of Epo. (*B*) Histone acetylation of H2A.X at Lys120 is decreased by lamin-B1 knockdown. (*C*) HSP90 and histone acetyltransferase inhibitors stiffen nuclei in erythropoiesis. GPA^{+} erythroblasts were treated with the HSP90 inhibitor 17-AAG (60 nM) or with the histone acetyltransferase inhibitor anacardic acid (A.A., 20 μM) for 1 d, followed by micropipette aspiration of nuclei. Although $GPA^{+/hi}$ cells generally have stiffer nuclei than GPA^{lo} (ProEry), all nuclei largely flow irreversibly at constant pressure. Both drugs phenocopy the stiffening of erythroblast and the decrease in lamin-B. Nuclear compliance change with the power law fit (*a, b*): (DMSO: 4.1, 0.14), (17-AAG 60 nM: 1.9, 0.09), [Anacardic Acid (A.A.) 10 μM: 1.9, 0.05] $P < 0.05$ ($n = 5$), DMSO vs. 17-AAG or A.A. for each time point in paired *t* test. (*Inset*) Graph shows down-regulation of lamin-B with both 17-AAG and A.A. One-way ANOVA $*P < 0.05$, Mean ± SD. (Scale bars: 3 μm.)

1. Hu J, et al. (2013) Isolation and functional characterization of human erythroblasts at distinct stages: Implications for understanding of normal and disordered erythropoiesis in vivo. *Blood* 121(16):3246–3253.
2. Grebenová D, et al. (2006) The proteomic study of sodium butyrate antiproliferative/cytodifferentiation effects on K562 cells. *Blood Cells Mol Dis* 37(3):210–217.
3. Kurokawa M, Zhao C, Reya T, Kornbluth S (2008) Inhibition of apoptosome formation by suppression of Hsp90beta phosphorylation in tyrosine kinase-induced leukemias. *Mol Cell Biol* 28(17):5494–5506.

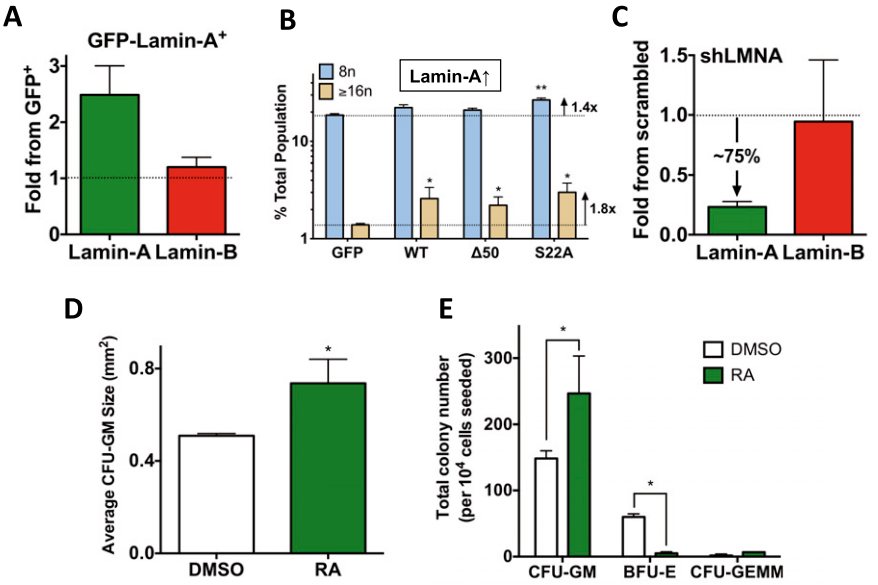

Fig. S6. (*A*) GFP–lamin-A overexpression increases lamin-A by 2.5-fold compared with GFP control ($n = 3$ donors, $P < 0.05$, mean ± SEM). (*B*) Lamin-A enhances MK polyploidization. Overexpression of GFP, wild-type (WT), Progerin mutant (Δ50), and phospho-deficient (S22A) mutant of lamin-A in MEG01 cells. $^{**}P < 0.05$, GFP vs. S22A 8n. $^{*}P < 0.05$, GFP vs. WT, Δ50 or S22A ($n = 4$). (*C*) Lamin-A shRNA down-regulates lamin-A selectively by 75% whereas lamin-B remains unchanged ($n = 3$ donors, $P < 0.05$, mean ± SEM). (*D*) Retinoic acid increases the mean size of CFU-GM. (*E*) Retinoic acid increases the number of CFU-GM whereas it decreases that of BFU-E ($n = 2$ donors, $P < 0.05$, mean ± SEM).

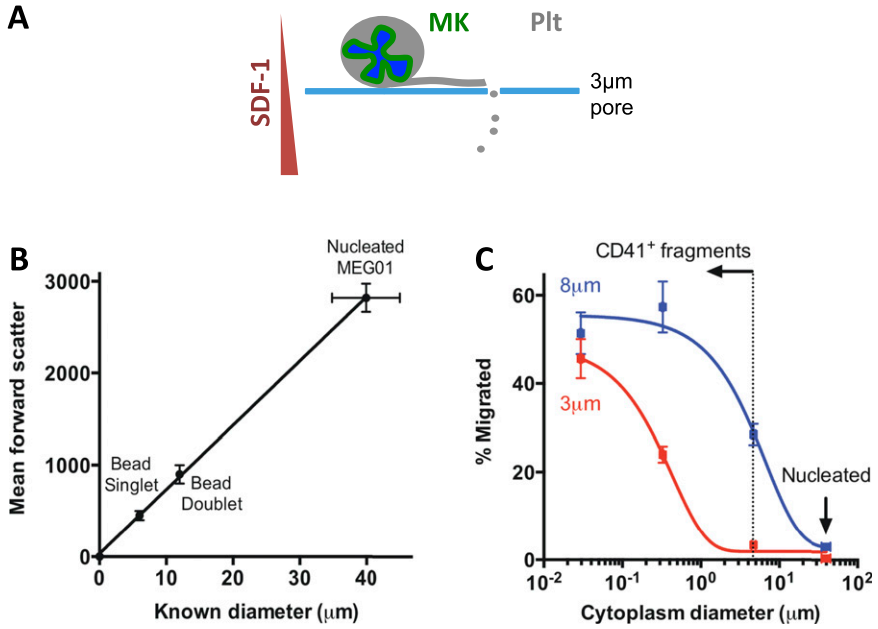

Fig. S7. Migration of nucleated MKs and platelet fragments through pores. (*A*) Illustration of nucleated MKs and platelets (plt) migrating through 3-μm pores under SDF-1 gradient. (*B*) Size calibration between forward scatter values from flow cytometry and known diameter of beads and MEG01 cells (measured by light microscopy), assuming that each cell or fragment is circular. Mean ± SEM, $n = 3$. (*C*) Migration of $CD41^{+}7\text{-}AAD^{-}$ fragments and nucleated cells from MEG01 through 3- and 8-μm pores. Cytoplasm diameter was extrapolated as in *B* assuming that each fragment or nucleated cell is circular. Exponential decay fit, half-life: 3-μm pore = 0.3 μm, 8-μm pore = 4.6 μm. $R^2 > 0.98$, mean ± SEM, $n = 3$.

Table S1. Lamin-A and lamin-B expression values calibrated by MS-IF

Cell type	Lamin-A	Lamin-B	A:B	A+B	A:C (WB)
A549	2.30	1.00	2.3*	3.30	0.78 ± 0.06
MSC	4.95	4.10	1.20	9.05	1.1
$CD34^+CD38^-$	0.27 ± 0.02	1.00 ± 0.03	0.28	1.27	1.6
$CD34^+CD38^+$	0.55 ± 0.06	1.51 ± 0.03	0.37	2.06	
ProEry	2.05 ± 0.10	0.58 ± 0.01	3.54	2.63	0.17
LateEry	1.07 ± 0.00	0.05 ± 0.01	19.66	1.12	0.95
MKP	2.75 ± 0.41	1.20 ± 0.17	2.28	3.95	N/A
MK	6.09 ± 0.79	3.39 ± 0.53	1.79	9.48	N/A
BM M	0.58 ± 0.25	0.24 ± 0.04	2.44	0.82	N/A
BM G	0.64 ± 0.03	0.58 ± 0.18	1.09	1.22	N/A
B Cell	0.18 ± 0.11	0.19 ± 0.08	0.96	0.37	N/A
T Cell	0.27 ± 0.11	0.38 ± 0.11	0.71	0.65	N/A
PB G/M	0.34 ± 0.13	0.54 ± 0.17	0.62	0.88	N/A

*Mass spectrometry measurement.

Table S2. Percentage of nucleated hematopoietic lineages in marrow and blood

	% of leukocytes		
Cell type	Marrow	Blood	Refs.
T cell	9.8	25	1, 2
B cell	3.3	4	1, 2
$CD33^{mid}$ (gran)	50.0	70	1, 2
$CD33^{hi}$ (mono)	10.0	5	1, 2
Nucleated erythroid	28.5	Very low	1, 2
Nucleated MK	1.3	Very low	2
$CD34^+$	0.8	0.06	3,4

1. Fauci AS, et al., eds (2009) *Harrison's Manual of Medicine* (McGraw-Hill, New York), 17th Ed.
2. Lee GR, et al., eds (1999) *Wintrobe's Clinical Hematology* (Lippincott Williams & Wilkins, Baltimore), 10th Ed.
3. McKenna DH, Jr, et al. (2010) CD34(+) cell selection using small-volume marrow aspirates: A platform for novel cell therapies and regenerative medicine. *Cytotherapy* 12(2):170–177.
4. Anonymous (2012) *Frequencies of Cell Types in Human Peripheral Blood* (StemCell Technologies, Vancouver, BC, Canada).

Table S3. Concentration of total nucleated hematopoietic cells in marrow and blood

Measurement	Marrow	Blood	Marrow/blood	Refs.
Nucleated cells/mL, $\times 10^7$	2.5	0.75	3.33	1, 2
Total volume, mL	541	5,000	0.11	3

1. McKenna DH, Jr., et al. (2010) CD34(+) cell selection using small-volume marrow aspirates: A platform for novel cell therapies and regenerative medicine. *Cytotherapy* 12(2):170–177.
2. Hoffman R, et al., eds (2008) *Hematology: Basic Principles and Practice* (Elsevier, Philadelphia), 5th Ed.
3. Sambuceti G, et al. (2012) Estimating the whole bone-marrow asset in humans by a computational approach to integrated PET/CT imaging. *Eur J Nucl Med Mol Imaging* 39(8): 1326–1338.

Table S4. Total estimated number of nucleated hematopoietic lineages in marrow and blood

Cell type	Cell no., $\times 10^7$		
	Marrow	Blood	Marrow/blood
Total nucleated	1,353	3,750	0.36
T cell	133	938	0.14
B cell	44	150	0.30
$CD33^{mid}$ (gran)	676	2,625	0.26
$CD33^{hi}$ (mono)	135	188	0.72
Nucleated erythroid	385	Close to 0	Close to ∞
Nucleated MK	17	Close to 0	Close to ∞
$CD34^+$	10	2	4.63

Table S5. Mass spectometry measurement of lamin B1 and B2 expression levels in a range of hematopoietic and cultured cell lines

Cell type	Lamin B1:B2 (median ion current)	Lamin B1: B2 (peptide count)	LMNB1 Wb	LMNB2 Wb
$CD34^+$	4: 1	18: 9	◎	◎
EPO	6: 1	ND	ND	ND
Pro	20: 1*	19: 0	ND	ND
E Baso	30: 1*	21: 0	ND	ND
L Baso	35: 1*	24: 0	ND	ND
Poly	3: 1	24: 12	ND	ND
Ortho	4: 1	17: 5	ND	ND
TPO	8: 1	ND	ND	ND
MEG01	3: 1	14: 1	◎	C
MKP	Lamin B2 not detected	6: 0	ND	ND
MK	Lamin B2 not detected	6: 0	ND	ND
MSC	0.7: 1	4: 6	◎	C
U251	1.6: 1	19: 12	●	◎
A549	1.8: 1	17: 10	●	◎

Proteins detected in mass spectometry experiments were quantified in two ways: by counting the number of tryptic peptides uniquely derived from each lamin isoform ("peptide count") and by comparing the median signal strength of those peptides ("median ion current"). Both methods give approximate and generally comparable measures of relative protein concentration, and as lamin-B1 and -B2 are of similar size and detectability, ratios of these values give an estimate of the lamin-B1: B2 composition. In samples where low levels of lamin-B2 became difficult to detect, the MS spectra were aligned with those from an A549 standard sample to record the ion currents. Where sufficient cell lysate was available, MS measurements were validated by qualitative WB using antibodies specific to lamin-B1 or B2. Although both B-type lamins show similar detectability in cultured cell lines, lamin-B1 becomes dominant during hematopoietic differentiation. ND, not determined; ○, no band; ◎, weak; ●, strong. EPO, Epo-cultured $CD34^+$-derived cells; Pro, proerythroblast; E Baso, early basophilic erythroblast; L Baso, late basophilic erythroblast; Poly, polychromatic erythroblast; Ortho, orthochromatic erythroblast; TPO, Tpo-cultured $CD34^+$-derived cells; MKP, megakaryocyte progenitors; MK, megakaryocytes; MSC, mesenchymal stem cells.
*Lamin B2 only detected with alignment.

Table S6. Representative images showing results from Western blot validation of lamin B1 and B2 expression levels

	MSC	U251	A549	MEG01	CD34$^+$
LMNB1		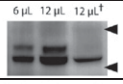			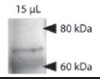
LMNB2